Comparison of hyperspectral imaging techniques for the elucidation of falsified medicines composition

Laureen Coic[a,1*], Pierre-Yves Sacré[a,1], Amandine Dispas[a], Abdoul Karim Sakira[a,c], Marianne Fillet[b], Roland D. Marini[a], Philippe Hubert[a], Eric Ziemons[a]

[a] University of Liege (ULiege), CIRM, VibraSanté Hub, Department of Pharmacy, Laboratory of Pharmaceutical Analytical Chemistry, CHU, B36, 4000 Liege, Belgium

[b] University of Liege (ULiege), CIRM, Laboratory of the Analysis of Medicines, Department of Pharmacy, CHU, B36, 4000 Liege, Belgium

[c] Université Ouaga 1 Pr Joseph KI-ZERBO, Ouagadougou, Burkina Faso

Abstract

Hyperspectral imaging has shown a high potential to analyze falsifications of solid pharmaceutical products since the last decade. Thanks to the non-destructive, ecological and non-invasive properties, it is a preferred technique for these kinds of applications. Moreover, thanks to the spectroscopic properties, it is possible to detect as well organic compounds as inorganic compounds in a single analysis. Therefore, we recommend using it as second-line laboratory analysis technique. Raman microscopy and Fourier Transform Infrared (FT-IR) microscopy are two interesting techniques that are complementary.

In this study, the potential of the two hyperspectral imaging techniques is evaluated to elucidate the composition of falsified antimalarial tablets. Hyperspectral data are analyzed by Multivariate Curve Resolution-Alternating Least Square (MCR-ALS). The results obtained from this study show that Raman hyperspectral imaging seems to be more suited to detect low dosed compounds possibly due to a smallest sampling volume. It has been also possible to link formulations of falsified samples of two different brands.

Keywords:

FT-IR spectroscopy; Raman spectroscopy; hyperspectral imaging; falsification; antimalarial

[1]These authors have equally contributed to this article.

*Corresponding Author. Tel.: +32 43664324; Fax: +32 43664317

E-mail address: laureen.coic@uliege.be and pysacre@uliege.be

Address: Laboratory of Pharmaceutical Analytical Chemistry, CIRM, Department of Pharmacy, University of Liege, B36, B-4000 Liège, Belgium

Introduction

Since the last decade, falsified medicines have been a burden for low and middle income countries (LMIC) [1]. Because of the increase of online trading and the lack of laws in some countries, pharmaceutical solid formulations are the best target for falsification. Several conventions, notably MEDICRIME in 2010 [2], have really helped to understand and apply laws creating the notion of "Pharmaceutical crime". New low-cost tools have been used to fight against falsification, such as the 2D barcodes or the Radio Frequency Identification (RFID) [3] on the outside packaging. It is already known that Africa is the continent that contains the most falsifications and the poorest quality drugs. Countries like Rwanda had the opportunity to be funded by the US's government's department United States Agency International Development in 2009 [4] and by Non-Governmental Organizations in 2011 [5] *interalia*. Since then, some strategies have been elaborated to control drug quality. For example, Rwanda prohibited antimalarial drug sales through private pharmacies in order to have public pharmacy monopoly. The Ministry of Health of Rwanda created a "Guideline for pharmacovigilance and medicine information system" in 2011 [6]. Nevertheless, other countries still know a growth of falsified drugs and an increasing mortality rate.

Many fatal diseases affect LMIC like malaria, which devastates people. Low quality medicines constitute a double burden since it does not treat patients and it increases resistance. Indeed, the low dose of active pharmaceutical ingredient (API) induces a rise of drug resistance and weakens the whole antimalarial therapeutic efficacy [7]. The Nigerian National Agency for Food and Drug Administration and Control (NAFDAC) has identified well known Coartem®(artemether/lumefantrine 20/120 mg) (batch number NOF 2153 and F2261) in 2011[8]. All of these drugs are still currently found on the African market with different expiry dates but still the same batch number. It was found in Democratic Republic of the Congo [9], Cameroon [10], Equatorial Guinea [11] and the last one was discovered the June 26th 2018 in Ghana with an expiry date of 05/2020 for the Coartem® F2153 and 03/2020 for Coartem® F2261 [12]. At the moment, some African countries possess some basic analytical tools, like thin layer chromatography (TLC) or the GPHF Minilab™, to establish if an antimalarial drug is falsified, but it is time consuming and requires consumables. Since several years, a few number of laboratories have developed new analytical methods such as high pressure liquid chromatography (HPLC) [13] or low-cost devices [14] to check the composition of antimalarial

tablets. Some works are still in progress to improve those methods thanks to the design space approach [15]. The implement of these types of method is rather difficult because of the high cost of analysis, due to the solvents, electricity and gas needed. Moreover, there is a lack of skilled labor to ensure the analysis. That is why several spectroscopic methods have been developed in parallel [16].

Indeed, vibrational spectroscopy is an analytical technique that has known a genuine expansion since two decades because of its interesting properties and the relevant information obtained. Some works have already been conducted on falsified medicines by near infrared spectroscopy, mid-infrared spectroscopy or Raman spectroscopy [17–19]. These analytical techniques requires no sample preparation (except surface milling) and can be applied on different type of molecules and physico-chemical forms. Furthermore, they are non-invasive, non-destructive and environment-friendly. However, spectral data have to be managed with chemometric tools and multivariate analysis. Most of the time, no database is accessible to make a comparison with the data obtained from analysis, so the database has to be done by itself. On the field, using handheld Raman spectrophotometers can quickly highlight suspicious counterfeit medicines, even through translucent containers [20]. Handheld devices can be used at any step of the supply chain to control drugs. Meanwhile, this type of analysis can only give preliminary conclusions regarding the API's presence or absence for example. That is why Raman spectroscopy has been coupled with a microscope to obtain more information. Some studies have been conducted on the screening of falsified drugs with Raman chemical imaging [21,22]. What is more, it has been demonstrated that a direct classical least square (DCLS) applied on the multivariate curve resolution – alternating least squares (MCR-ALS) pure spectrum matrix can be used to obtain semi-quantitative information about the tablet's composition.

In the pharmaceutical field, applications of FT-IR imaging, especially in reflection mode were not found in the literature, FT-IR imaging is usually performed with an attenuated total reflectance (ATR) accessory. It has been shown to be a powerful technique to analyze co-crystal formulation [23] or even to study the interconversion between the crystalline forms of nimodipine[24]. A study has been done on the classification of falsified Viagra® and Cialis®[25], showing that, with the help of chemometrics, mid-infrared spectroscopy can be an efficient tool to discriminate conform from falsified drugs. ATR imaging of pharmaceutical samples also helped analyzing tablet dissolution [26,27]. FT-IR microscopy is not a commonly used technique because of the relatively high cost of the instrument. However, it could be an

interesting alternative to the Raman microscopy. Indeed, the latter suffer from auto fluorescence of samples that is mainly present in colored samples or due to high amount of impurities.

The aim of this study was to compare the potential of the FT-IR chemical imaging versus Raman chemical imaging to elucidate the whole composition of a falsified tablet. The first step was to carry out FT-IR and Raman chemical imaging analyses on falsified and reference tablets and to apply the MCR-ALS algorithm to extract the pure compound spectra. A comparison study between results of each technique was performed, in order to try to establish a link between supposed Coartem® Novartis and Combiart® Strides Arco Labs medicines. Thanks to the combination of spectroscopy and imaging as sampling technique, essential information on chemical composition were obtained, which provide the fingerprint of a falsified medicine production.

Experimental

Samples

Genuine sample of Coartem® was purchased from a local pharmacy in Belgium under the brand name Riamet® (batch X0136 exp: APR 2019), G1 and G2 (see Table 1).

Falsified samples were seized by the Ministry of Health in Democratic Republic of Congo. Two batches of Coartem® and two batches of Combiart tablets were analyzed: S1, S2, S2 and S4 (see Table 1). For each batch, three samples were analyzed in order to have a good representativeness of the production.

A supplementary tablet of falsified Coartem® seized by the Beninese Ministry of Health in 2014 was analyzed. (Batch F2261; Mfd 01-2014; exp: 02-2018). This sample was analyzed in a previous study [28].

Before being analyzed by FT-IR and Raman imaging, tablets were glued on a microscope slide and their surface was milled using a Leica EM Rapid milling system equipped with a tungsten carbide miller (Leica Microsystems GmbH, Wetzlar, Germany).

FT-IR Microscope

The Fourier transform infrared hyperspectral imaging data was acquired with a FT-IR Cary 670/620 Agilent series microscope (Agilent Technologies) equipped with a 15x infrared objective, with a numerical aperture (NA) of 0.62 and a FPA (64x64) detector. The software used for the acquisition is Resolution Pro from Agilent Technologies. The imaging acquisition

gives a spatial resolution of 5.5µm. All the acquisitions are performed in reflection mode, with a resolution of 8 cm^{-1}over a spectral range of 850-4000 $cm^{-1}$and 16 co-added scans.

The reference database spectra were obtained compressing raw materials with a Specac 12 mm die, with 5-ton compression.

Raman microscope

Raman hyperspectral imaging analyses of the samples were performed with a Labram HR Evolution (Horiba scientific) equipped with an EMCCD detector (1600×200 pixel sensor) (Andor Technology Ltd.), a Leica 50x Fluotar LWD objective and a 785 nm laser with a power of 45mW at sample (XTRA II single frequency diode laser, Toptica Photonics AG).

A 300 gr/mm grating fixed at 1200 cm^{-1} (spectral range of 464–1853 cm^{-1}) was used to perform the mappings with a double acquisition of 1 sec. The confocal slit-hole was fixed at 200 µm. The spectra were collected with the LabSpec 6 (Horiba Scientific) software.

The whole tablet surface was mapped with a step size of 60 µm.

Data pre-processing

The FT-IR data were corrected by two pre-processing. First, an Asymmetric Least Square baseline correction (p: $1x10^{-5}$, λ: $3x10^{4}$) has been applied. Then, a Kubelka-Munk correction [30] was used to correct the spectrum. As with Raman analysis, an MCR-ALS analysis was applied with non-negativity on concentration and spectra as constraints.

The Raman data were corrected by an Asymmetric Least Square baseline correction (p: $1x10^{-5}$, λ: $3x10^{4}$) [29]. The pre-processed data were then analysed by MCR-ALS. In order to detect as much compounds as possible, three MCR-ALS models were successively done with 10, 30 and 50 components respectively. The number of MCR components to be resolved was fixed and not optimized for each sample in order to have a generic strategy that could be applied to any new sample. Major compounds (e.g. lumefantrine) are better resolved with less component MCR models while minor compounds (e.g. magnesium stearate) are better resolved by higher component MCR models. Non-negativity on concentration and spectra were used as constraints.

FT-IR data are heavier than Raman ones, because the FPA provide a fixed size of mosaic that gives a hypercube of 64x64x819 data points per mosaic. Because of the size of tablets, approximately more than 1x1 cm^{2}, an image can represent almost 60 GB of data. Analyses

performed on CPU often ran out of memory. An alternative to manage such data size consists in decomposing each image into 16 smaller images that are easier to analyse using less memory. MCR-ALS is applied on each small image with a variable number of component.

Regarding the database, a homemade Matlab function has been created to match unknown spectrum with any type of reference database and wavenumbers range. Reference spectra used in this study are provided in supplementary data (Table S1).
All computations were carried out with Matlab R2018a (The Mathworks) and MCR-ALS have been performed with the PLS Toolbox (version 8.6.2, Eigenvector Research).

Theory

Multivariate Curve Resolution – Alternating Least Square (MCR-ALS)

The hyperspectral data are represented as a hypercube (*x*,*y*,*z*), where *x* and *y* are the pixel coordinates and *z* is the spectral coordinate. The MCR-ALS algorithm is based on the assumption Beer-Lambert law is respected; it means that each pixel is equal to the concentration-weighted sum of the contributions of the pure spectra of the image. Because hyperspectral data are multivariate data, the Beer-Lambert law is written as follow (Eq.1):

$$\mathbf{D=C.S^T + E} \quad (1)$$

where C is the matrix of the relative concentration profiles of the components of the image, S the matrix of pure spectrum and E, the residual matrix containing the experimental error which does not originate from the sample under examination. This model is built via the alternating least square iterative algorithm, which consists of three steps. First, the operator has to indicate the number of supposed component in D. It can be initialized via a preliminary principal component analysis or by the SIMPLISMA algorithm [31]. After this step, initial estimate of the S^T matrix is done. Finally, several constraints have to be fixed for the optimization step until the convergence. It is for example the non-negativity constraint on spectra or on the contribution. As part of this study, these two constraints were applied. In the end of the iteration algorithm, the two matrices are calculated as follow (Eq.2, Eq.3):

$$\mathbf{C=D.S(S^T.S)^{-1}} \quad (2)$$

$$\mathbf{S=(C^T.C)^{-1}C^T.D} \quad (3)$$

Thanks to the two matrices, the scores and loadings MCR are gathered. The information that will be used for this study is the loadings matrix.

Hit Quality Index

In the study, the MCR-loadings were matched with a handmade previously built database thanks to a hit quality index (HQI) [32](Eq.4).

$$HQI = \frac{(\overrightarrow{Standard} \cdot \overrightarrow{Unknown})^2}{(\overrightarrow{Standard} \cdot \overrightarrow{SStandard}) \times (\overrightarrow{Unknown} \cdot \overrightarrow{Unknown})} \quad (4)$$

This statistic tool provides the spectral correlation between a reference and an unknown sample. The HQI gives a number between 0 and 1. The closer to HQI=1, the more correlated is the unknown spectrum with the library.

Results and discussion

Regarding FT-IR analysis, the studied range of wavenumbers was reduced to the fingerprint region (850-2000 cm^{-1}). Indeed, using the entire range has a bad incidence of the MCR results. Most loadings are related to the upper range signal and mask the useful information mainly present in the fingerprint region. The OH region is large and intense it has too much weigh on variability.

The results of the analysis of reference tablet are rather the same comparing both techniques. Results are described in Table 2 for the FT-IR analysis and in Table 3 for the Raman analysis. The decomposition of the FT-IR data shows that it is composed of artemether, lumefantrine, and hypromellose, with a HQI > 0.70. The results obtained from the small images have improved the resolution. Indeed, microcrystalline cellulose has been found with a HQI > 0.90 whereas it was not detected based on the whole map. Meanwhile, the Raman data decomposition shows that it is composed of artemether, lumefantrine, microcrystalline cellulose, magnesium stearate with a HQI > 0.70. Raman microspectroscopy seems to be more sensitive to detect low dosed molecules than FT-IR. The spatial repartition of each compound is represented in the Figure 1 for FT-IR and in the Figure S1 for Raman. It allows having an idea about the spatial distribution and the proportion of each chemical compound along the tablet.

Regarding the falsified tablets, loadings obtained from both FT-IR and Raman systems show that starch and calcium carbonate are the main constituents of all formulations. Titanium dioxide (TiO_2) has two polymorphic forms, rutile and anatase. Anatase was not found during this study since their absorption bands are below 850 cm^{-1} and therefore not accessible to us. Rutile, on the other hand, has a broad absorption band around 1000 cm^{-1}. However, this band

is so broad that it was very likely eliminated by the baseline correction. On the contrary, TiO_2 polymorphs have a strong Raman signature enabling an easy identification. An example of matching between loadings and reference spectrum are shown in Figure 2 for the FT-IR technique.

Raman mapping also detected the presence of talc and two unexpected API's: sildenafil citrate and ciprofloxacin hydrochloride monohydrate. Sildenafil citrate is classically used for erectile dysfunction and ciprofloxacin hydrochloride monohydrate is a fluoroquinolone family antibiotic. This is an unexpected and worrying result for an antimalarial drug. Indeed, the presence of an antibiotic can induce a future resistance for what the antibiotic is normally used.

Comparison between FT-IR and Raman microscopy

Regarding results obtained for each technique, it appears that there is a significant difference between both in terms of sensitivity. It may be explained by the difference of spatial resolution between the FT-IR and Raman equipment configuration. Indeed, the actual configuration of the Raman system provides a theoretical spot size of ~2 µm, which increases the possibility of measuring the spectrum of a pure compound. Whereas, FT-IR imaging measures the mean spectrum over a surface of 5.5 µm of diameter. This spectrum may induce a loss of information. A 25x IR objective with a higher NA (0.81) was tested. The resolution is better with 3.3 µm of lateral resolution. New molecules have been detected such as magnesium stearate and a coloring agent (possibly tartrazine) in falsified tablets (Figure 3). The last compound is interesting because, falsified tablets are yellow colored to mimic the presence of lumefantrine. The coloring agent was also detected in Raman imaging but its identity remains unclear since several coloring agents have nearly the same spectrum (tartrazine and magnesium euxanthate). That is why, more investigation should be performed to confirm the identity of this compound and add it to the reference database.

After this first investigation, it seems that Raman hyperspectral imaging is more appropriated for the composition elucidation of falsified tablets. Indeed, the difference of data size between the two techniques (150 Mo for Raman mapping and from 9 GB to 60 GB for FT-IR data), the total analysis time (data acquisition ~11h for a whole tablet and processing) are favorable to Raman spectroscopy. For instance, data processing takes much more time with FT-IR data, approximately 5 hours compared to Raman ones which can take approximately 2 hours. Some new strategies have to be developed to find a way to reduce time consuming with FT-IR analysis such as GPU analysis. In addition, other pre-processing techniques such as the Kramers-Krönig

transform may be interesting to suppress the specular reflection that masks the signal of interest. The long analysis time may be shortened depending on the sought information. Indeed, for a first screening, the analysis may be shortened to several minutes but, in the present case, we wanted to find as much compounds as possible. Therefore, we optimized spectral signal rather than analysis time. Furthermore, this approach is envisaged to be performed on already confirmed falsified samples to obtain information on both organic and inorganic compound without sample destruction.

Another major interesting result of this study is the link that may be inferred between several falsification cases. Indeed, ciprofloxacin hydrochloride monohydrate and citrate sildenafil are present in most of the formulation besides excipients such as talc, titanium dioxide, calcium carbonate, starch and a coloring agent. The identification of particular polymorphs or salts of API/excipients may constitute a specific fingerprint of a production. Because Raman and FT-IR analysis are performed in reflection mode, the surface of analysis has a significant incidence on the elucidation of the composition. The absence of detection of sildenafil citrate in some tablets is possibly due to the non-homogeneity of the samples. This point constitutes a major limitation to the present approach. Indeed, control laboratories often have few tablets to analyze and it is impossible to ensure that the analysis of the surface of one (or even three) tablets is representative of the whole production. Nevertheless, this may provide information on the production and may possibly link several falsified samples, as it was the case in our study. Besides these considerations on sample homogeneity, it may also provide a first insight in the tablet composition (organic and inorganic) to guide and rationalize further analyses (e.g. identity confirmation with mass spectrometry).

Conclusion

The potential of hyperspectral imaging for the analysis of falsified medicines has already been demonstrated. During this research, we emphasize on the possibility to elucidate the complete composition of falsified tablets. Indeed, vibrational spectroscopy is able to detect in a single analysis both organic and inorganic compounds being also sensitive to solid states and salt forms. The elucidated composition may then be used as a fingerprint of the production and could be used to complete the forensic investigations.

Furthermore, thanks to the non-destructive character of this kind of analysis, it may be performed as first laboratory screening to prepare the further depth analysis of the samples (e.g. mass spectrometry, NMR, etc.). It may also give some answers to an urgent question: what is the patient's risk taking this medicine.

Several technologies and equipment configurations exist on the market. In this study, we investigated two complementary techniques: FT-IR imaging in reflection mode and Raman imaging. Using default configurations of the equipment, Raman microspectroscopy outperformed FT-IR imaging in terms of both elucidated compounds but also analysis time and data size. However, several options are under investigation to enhance FT-IR performances in this context. Indeed, some samples may not be analyzed by Raman microspectroscopy due to a high auto fluorescence background and may therefore be analyzed by FT-IR imaging.

Acknowledgments

This project has been supported by the European funds of regional development (FEDER) and by Walloon as part of the operational program "Walloon-2020.EU".

The financial support of this research by the Walloon Region of Belgium in the framework of the Vibra4Fake project (convention n°:7517) is gratefully acknowledged.

References

[1] W.L. Hamilton, C. Doyle, M. Halliwell-Ewen, G. Lambert, Public health interventions to protect against falsified medicines: a systematic review of international, national and local policies, Health Policy Plan. 31 (2016) 1448–1466. doi:10.1093/heapol/czw062.

[2] Council of Europe, The MEDICRIME Convention, (2011).

[3] WHO | WHO Member State Mechanism, WHO. (2018). http://www.who.int/medicines/regulation/ssffc/mechanism/en/ (accessed September 19, 2018).

[4] J. Nwokike, M.P. Joshi, Assessment of Pharmacovigilance and Medicine Safety System in Rwanda, 2009. www.msh.org/sps (accessed September 19, 2018).

[5] M.L. Heyman, R.L. Williams, Ensuring global access to quality medicines: Role of the US pharmacopeia, J. Pharm. Sci. 100 (2011) 1280–1287. doi:10.1002/jps.22391.

[6] D.A. ASIIMWE, Rwanda Pharmacovigilance Guidelines, (2010).

[7] P.N. Newton, C. Caillet, P.J. Guerin, A link between poor quality antimalarials and malaria drug resistance?, Expert Rev. Anti. Infect. Ther. 14 (2016) 531–533. doi:10.1080/14787210.2016.1187560.

[8] Circulation Of Fake Anti-Malaria Drugs – NAFDAC, (n.d.). https://www.nafdac.gov.ng/circulation-of-fake-anti-malaria-drugs/ (accessed September 19, 2018).

[9] O. ILUNGA KALENGA, RDC _Santé : ALERTE! COMMUNIQUE DU MINISTRE DE LA SANTE |, (2017). http://aicmonline.com/rdc-_sante-alerte-communique-ministre-de-sante/ (accessed September 19, 2018).

[10] E. ZIEMINE, Le Coartem en plaquette interdit, (2013). http://ct2015.cameroon-tribune.cm/index.php?option=com_content&view=article&id=77643:antipaludeens-le-coartem-en-plaquette-interdit&catid=4:societe&Itemid=3 (accessed September 19, 2018).

[11] H. Kaur, E.L. Allan, I. Mamadu, Z. Hall, M.D. Green, I. Swamidos, P. Dwivedi, M.J. Culzoni, F.M. Fernandez, G. Garcia, D. Hergott, F. Monti, Prevalence of substandard and falsified artemisinin-based combination antimalarial medicines on Bioko Island, Equatorial Guinea, BMJ Glob. Heal. 2 (2017) e000409. doi:10.1136/bmjgh-2017-000409.

[12] A. Basit, Fake Medicines For Malaria Uncovered, 2018. http://www.ghanalive.tv/2018/06/27/fake-medicines-malaria-uncovered/.

[13] L. Hoellein, U. Holzgrabe, Development of simplified HPLC methods for the detection of counterfeit antimalarials in resource-restraint environments, J. Pharm. Biomed. Anal. 98 (2014) 434–445. doi:10.1016/j.jpba.2014.06.013.

[14] R.D. Marini, E. Rozet, M.L.A. Montes, C. Rohrbasser, S. Roht, D. Rhème, P. Bonnabry, J. Schappler, J.L. Veuthey, P. Hubert, S. Rudaz, Reliable low-cost capillary electrophoresis device for drug quality control and counterfeit medicines, J. Pharm. Biomed. Anal. 53 (2010) 1278–1287. doi:10.1016/j.jpba.2010.07.026.

[15] B. Debrus, P. Lebrun, J.M. Kindenge, F. Lecomte, A. Ceccato, G. Caliaro, J.M.T. Mbay, B. Boulanger, R.D. Marini, E. Rozet, P. Hubert, Innovative high-performance liquid chromatography method development for the screening of 19 antimalarial drugs based on a generic approach, using design of experiments, independent component analysis

and design space, J. Chromatogr. A. 1218 (2011) 5205–5215. doi:10.1016/j.chroma.2011.05.102.

[16] J.K. Mbinze, P.-Y. Sacré, A. Yemoa, J. Mavar Tayey Mbay, V. Habyalimana, N. Kalenda, P. Hubert, R.D. Marini, E. Ziemons, Development, validation and comparison of NIR and Raman methods for the identification and assay of poor-quality oral quinine drops, J. Pharm. Biomed. Anal. 111 (2015) 21–27. doi:10.1016/j.jpba.2015.02.049.

[17] J. Coelho Neto, F.L.C. Lisboa, ATR-FTIR characterization of generic brand-named and counterfeit sildenafil- and tadalafil-based tablets found on the Brazilian market, Sci. Justice. 57 (2017) 283–295. doi:10.1016/j.scijus.2017.04.009.

[18] P.-Y. Sacré, E. Deconinck, T. De Beer, P. Courselle, R. Vancauwenberghe, P. Chiap, J. Crommen, J.O. De Beer, Comparison and combination of spectroscopic techniques for the detection of counterfeit medicines, J. Pharm. Biomed. Anal. 53 (2010) 445–453. doi:10.1016/j.jpba.2010.05.012.

[19] H. Rebiere, C. Ghyselinck, L. Lempereur, C. Brenier, Investigation of the composition of anabolic tablets using near infrared spectroscopy and Raman chemical imaging, Drug Test. Anal. 8 (2015) n/a-n/a. doi:10.1002/dta.1843.

[20] D.I. Ellis, R. Eccles, Y. Xu, J. Griffen, H. Muhamadali, P. Matousek, I. Goodall, R. Goodacre, Through-container, extremely low concentration detection of multiple chemical markers of counterfeit alcohol using a handheld SORS device, Sci. Rep. 7 (2017) 1–8. doi:10.1038/s41598-017-12263-0.

[21] H. Rebiere, M. Martin, C. Ghyselinck, P.-A. Bonnet, C. Brenier, Raman chemical imaging for spectroscopic screening and direct quantification of falsified drugs, J. Pharm. Biomed. Anal. 148 (2018) 316–323. doi:10.1016/j.jpba.2017.10.005.

[22] P.-Y. Sacré, E. Deconinck, L. Saerens, T. De Beer, P. Courselle, R. Vancauwenberghe, P. Chiap, J. Crommen, J.O. De Beer, Detection of counterfeit Viagra® by Raman microspectroscopy imaging and multivariate analysis, J Pharm Biomed Anal. 56 (2011) 454–461. doi:http://dx.doi.org/10.1016/j.jpba.2011.05.042.

[23] P. Barmpalexis, A. Karagianni, I. Nikolakakis, K. Kachrimanis, Artificial neural networks (ANNs) and partial least squares (PLS) regression in the quantitative analysis of cocrystal formulations by Raman and ATR-FTIR spectroscopy, J. Pharm. Biomed. Anal. 158 (2018) 214–224. doi:10.1016/j.jpba.2018.06.004.

[24] N.L. Calvo, N.M. Balzaretti, M. Antonio, T.S. Kaufman, R.M. Maggio, Chemometrics-assisted study of the interconversion between the crystalline forms of nimodipine, J. Pharm. Biomed. Anal. 158 (2018) 461–470. doi:10.1016/j.jpba.2018.06.019.

[25] A. Kahmann, M.J. Anzanello, F.S. Fogliatto, W.A. Chaovalitwongse, M.C.A. Marcelo, M.F. Ferrão, R.S. Ortiz, K.C. Mariotti, Interval importance index to select relevant ATR-FTIR wavenumber Intervals for falsified drug classification, J. Pharm. Biomed. Anal. 158 (2018) 494–503. doi:10.1016/j.jpba.2018.06.046.

[26] K.L.A. Chan, S. V Hammond, S.G. Kazarian, Applications of Attenuated Total Reflection Infrared Spectroscopic Imaging to Pharmaceutical Formulations, Anal Chem. 75 (2003) 2140–2146. doi:10.1021/ac026456b.

[27] P.S. Wray, G.S. Clarke, S.G. Kazarian, Dissolution of tablet-in-tablet formulations studied with ATR-FTIR spectroscopic imaging, Eur J Pharm Sci. 48 (2013) 748–757. doi:10.1016/j.ejps.2012.12.022.

[28] A. Yemoa, V. Habyalimana, J.K. Mbinze, V. Crickboom, B. Muhigirwa, A. Ngoya, P.-Y. Sacre, F. Gbaguidi, J. Quetin-Leclercq, P. Hubert, R.D. Marini, Detection of Poor Quality Artemisinin-based Combination Therapy (ACT) Medicines Marketed in Benin Using Simple and Advanced Analytical Techniques, Curr. Drug Saf. 12 (2017) 178–186. doi:10.2174/1574886312666170616092457.

[29] P.H.C. Eilers, H.F.M. Boelens, asymmetric least squares for baseline correction, (2005).

[30] W. Kessler, D. Oelkrug, R. Kessler, Using scattering and absorption spectra as MCR-hard model constraints for diffuse reflectance measurements of tablets, Anal. Chim. Acta. 642 (2009) 127–134. doi:10.1016/j.aca.2009.01.057.

[31] K. Kumar, Random Initialisation of the Spectral Variables: an Alternate Approach for Initiating Multivariate Curve Resolution Alternating Least Square (MCR-ALS) Analysis, J. Fluoresc. 27 (2017) 1957–1968. doi:10.1007/s10895-017-2132-0.

[32] Q. Gao, Y. Liu, H. Li, H. Chen, Y. Chai, F. Lu, Comparison of several chemometric methods of libraries and classifiers for the analysis of expired drugs based on Raman spectra, J. Pharm. Biomed. Anal. 94 (2014) 58–64. doi:10.1016/j.jpba.2014.01.027.

399 Figure 1 : FT-IR MCR scores and loadings for the S1 tablet

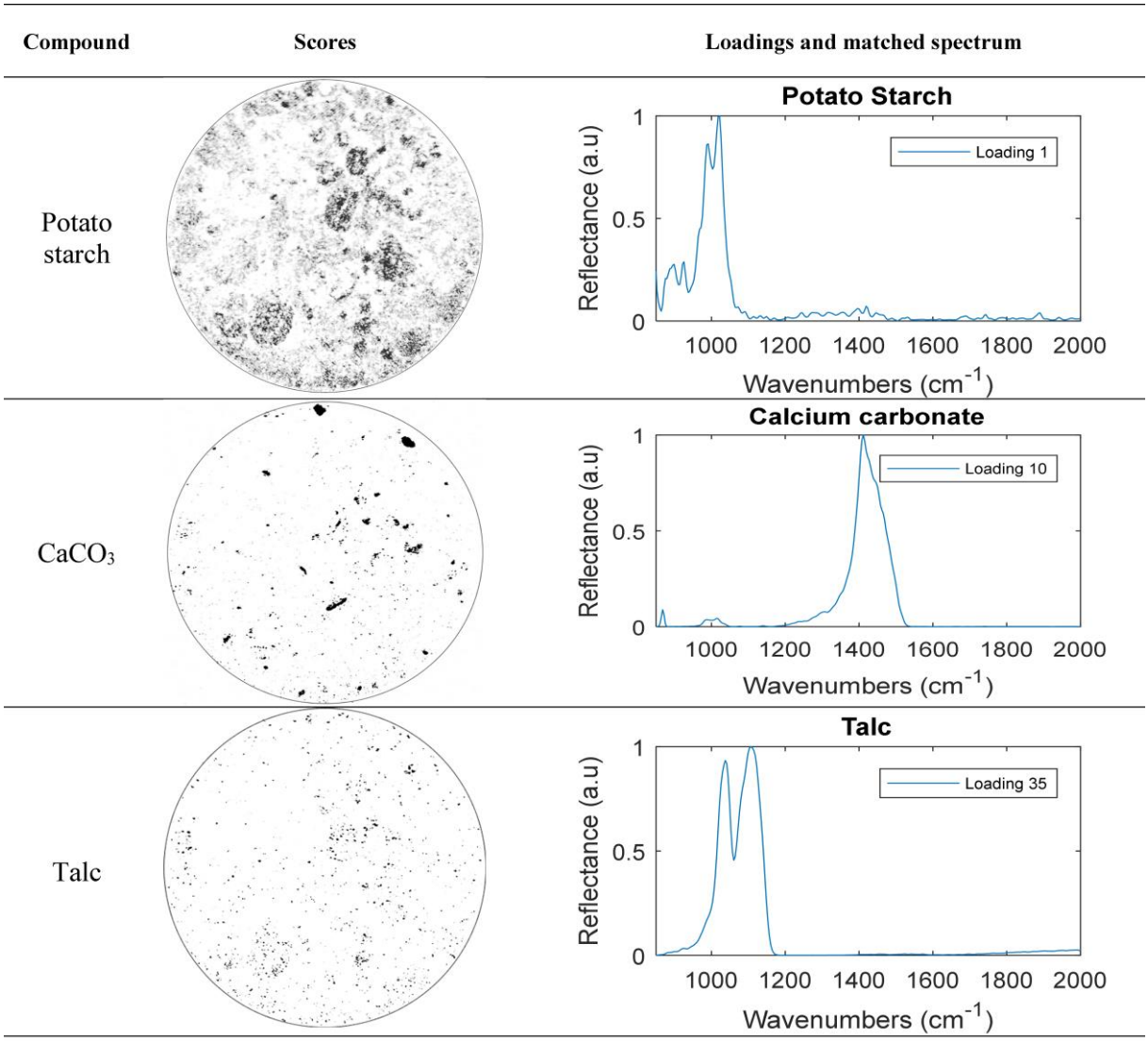

400

401

Figure 2 : MCR loadings match with the FT-IR reference database for the tablet S1. (a) potato starch, (b) magnesium stearate, (c) talc and (d) calcium carbonate.

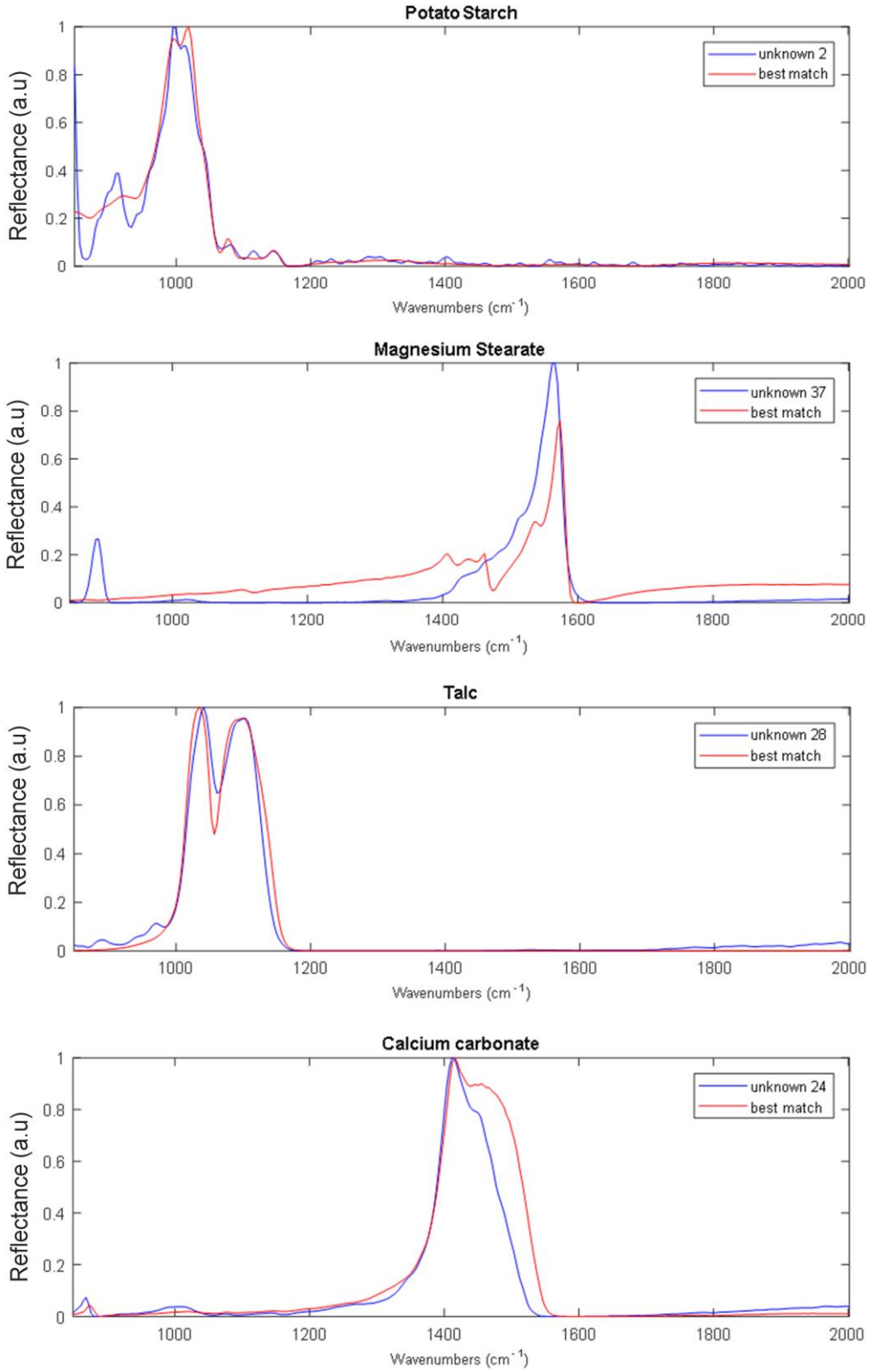

405 Figure 3 : MCR loadings for FT-IR imaging for the tablet S1 and match with the tartrazine
406 spectrum

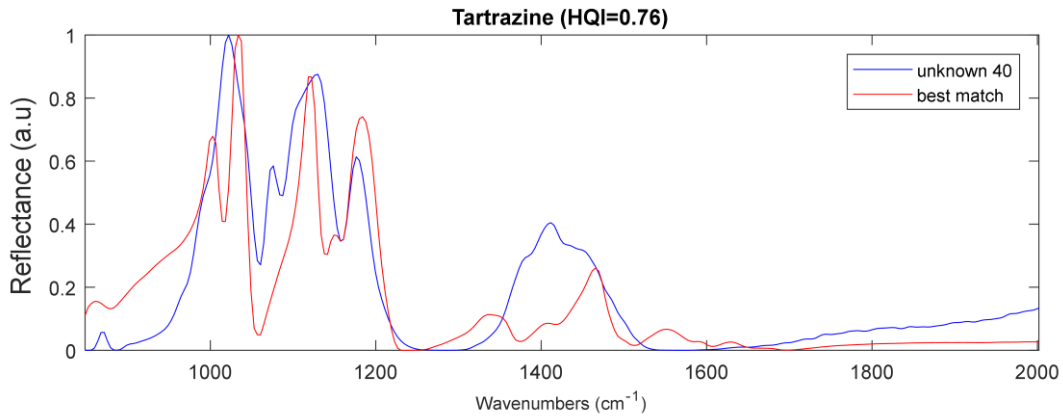

407

408

409 Table 1 : Samples description. In the “code” column, G is assigned for reference tablets and S
410 for samples

Authenticity	Code	Brand	Manufacturer	Batch number	Expiry date
Reference tablet	G1	Combiart	Strides Arco Labs	7227669	juin-18
Reference tablet	G2	Riamet	Novartis	X0136	apr-19
Falsified tablet	S1	Combiart	Strides Arco Labs	7225500	aug-19
Falsified tablet	S2	Combiart	Strides Arco Labs	7228051	juil-19
Falsified tablet	S3	Coartem	Novartis	F2153	nov-18
Falsified tablet	S4	Coartem	Novartis	F2153	juil-19
Falsified tablet	S5	Coartem	Novartis	F2261	feb-18

411

412 Table2 : Solving composition of artemether/lumefantrine formulation by FT-IR hyperspectral
413 imaging : matching with the database by using the HQI

FTIR microscope results	G1	G2	S1_R1	S1_R2	S1_R3	S2_R1	S2_R2	S2_R3	S3_R1	S3_R2	S3_R3	S4_R1	S4_R2	S4_R3	S5_R1
Artemether	0.9331	0.8289	-	-	-	-	-	-	-	-	-	-	-	-	-
Lumefantrine	0.8349	0.7254	-	-	-	-	-	-	-	-	-	-	-	-	-
Ciprofloxacin HCl.H2O	-	-	-	-	-	-	-	-	-	-	-	-	-	-	-
Sildenafil citrate	-	-	-	-	-	-	-	-	-	-	-	-	-	-	-
TiO2 (anatase)	-	-	-	-	-	-	-	-	-	-	-	-	-	-	-
TiO2 (rutile)	-	-	-	-	-	-	-	-	-	-	-	-	-	-	-
Talc	-	-	0.9779	0.9577	0.93	0.9702	0.8327	0.8938	0.8969	0.9103	0.9488	0.9621	0.917	0.9671	0.7246
Potato starch	0.9555	-	0.9743	0.9821	0.99	0.9955	0.9035	0.9549	0.9044	0.997	0.9529	0.9692	0.9813	0.903	0.9892
CaCO3	-	-	0.908	0.9715	0.87	0.8776	0.8802	0.9385	0.8816	0.9593	0.8754	0.8694	0.7176	0.897	0.9550
Magnesium stearate	-	-	0.6792	0.58	0.7063	-	-	-	-	0.5525	-	-	0.6156	0.6403	-
Microcrystalline cellulose	0.9541	0.9456	-	-	0.7391	-	-	-	-	-	-	-	-	-	-
Hypromellose	0.8226	-	-	-	-	-	-	-	-	-	-	-	-	-	-
D-Glucose	-	-	-	-	-	-	-	-	-	-	-	-	-	-	0.8545
Tartrazine	-	-	0.7624	0.6432		0.533	-	-	-	0.5682	-	-	-	-	-

414

415 Table3 : Solving composition of artemether/lumefantrine formulation by Raman hyperspectral
416 imaging : matching with the database by using the HQI

Raman microscope results	G1	G2	S1_R1	S1_R2	S1_R3	S2_R1	S2_R2	S2_R3	S3_R1	S3_R2	S3_R3	S4_R1	S4_R2	S4_R3	S5_R1
Artemether	0.91	0.73	-	-	-	-	-	-	-	-	-	-	-	-	-
Lumefantrine	0.99	0.98	-	-	-	-	-	-	-	-	-	-	-	-	-
Ciprofloxacin $HCl.H_2O$	-	-	0.97	0.92	0.93	0.96	0.93	0.92	0.91	0.95	0.95	0.84	0.93	0.91	-
Sildenafil citrate	-	-	0.96	0.78	0.71	-	0.75	-	0.86	-	0.82	-	0.79	0.81	-
TiO_2 (anatase)	-	-	-	-	-	0.94	-	-	-	0.88	-	-	-	0.92	-
TiO_2 (rutile)	-	-	0.93	0.94	0.98	0.86	0.97	0.98	0.98	0.98	0.97	0.86	0.99	0.98	-
Talc	-	-	0.95	0.98	0.99	0.99	0.97	0.97	0.96	0.98	0.95	0.98	0.98	0.96	-
Potato starch	-	-	0.98	0.97	0.95	0.98	0.96	0.94	0.95	0.97	0.97	0.92	0.97	0.94	0.95
$CaCO_3$	-	-	0.92	0.98	0.93	0.98	0.99	0.95	0.95	0.97	1.00	0.99	0.99	0.98	0.91
Magnesium stearate	0.72	-	-	0.75	0.86	0.86	0.88	0.74	-	0.82	0.79	0.77	0.81	0.78	0.85
Microcrystalline cellulose	0.76	0.96	-	-	-	-	0.80	-	-	-	-	-	-	-	-
Hypromellose	-	-	-	-	-	-	-		-	-	-	-	-	-	-
D-Glucose	-	-	-	-	-	-	-		-	-	-	-	-	-	0.96
Tartrazine	-	-	-	0.71	0.67	-	0.73	0.72		0.65	0.69	-	0.76	0.64	

417